JOURNAL OF MATERIALS SCIENCE **39** (2004) 1259– 1265

Structure stability of AA3003 alloy with ultra-fine grain size

Z. P. XING
Beijing Institute of Aeronautical Materials, Beijing 100095, People's Republic of China; Korea Institute of Machinery & Materials, 66 Sangnam-Dong, Changwon 641-010, Korea

S. B. KANG*, H. W. KIM
Korea Institute of Machinery & Materials, 66 Sangnam-Dong, Changwon 641-010, Korea
E-mail: sbkang@kmail.kimm.re.kr

The study on the structure stability of AA3003 alloy produced by an intense plastic straining process named accumulative roll bonding (ARB) has been conducted. The results show that continuous recrystallization took place in the ARBed 3003 alloy with increasing the annealing time at 250°C and increasing the annealing temperature to 275°C. While, discontinuous recrystallization began in some regions after 300°C annealing, and nearly finished after 400°C annealing. Furthermore, an unusual tensile behavior was observed in this alloy after annealing at 250–275°C. The Hall-Petch dependence was observed in the plot of microhardness versus $d^{-1/2}$ of the ARBed 3003 alloy, but its dependence slope was changed. The ultra-fine grains ($<1\ \mu$m) formed in the ARBed 3003 alloy can be stable until annealing at 250°C for 1 h, and the fine grains ($<2\ \mu$m) can be stable until annealing at 275°C for 1 h. Therefore, grain structure formed in the ARBed 3003 alloys after intense plastic strain is reasonably stable. In addition, the mechanism of structure stability and mechanical behavior were also discussed.

1. Introduction

Investigations conducted in recent years testify that a very high plastic strain can produce ultra-fine grain (UFG) materials. Several techniques are now available for producing high strains, including cyclic extrusion compression (CEC) [1], torsion straining under high pressure (TS) [2], equal channel angular press (ECAP) [3, 4], and accumulative roll bonding (ARB) [5–14]. Most of several-cycle ARB processed materials have structures with sub-micrometer grains and show very high strength at ambient temperature [5–8, 11, 14]. However, ARBed materials have the low tensile ductility at ambient temperature. This is an inherent limit for their practical application as other intense plastic straining materials. After ARB process, the specimens accumulated considerable residual stress induced by high dislocation density inside materials. The heat treatment for relieving residual stress is necessary for their practical uses. Furthermore, superplastic forming, which is the representative metal forming process using ultra fine grain (UFG) structure, is also a high-temperature process. In order to take the advantages of UFG materials including the mechanical superiority and high formability, UFG structure should be maintained stable under either heat processing conditions or the service conditions [15]. Previous investigation showed that UFGed 6061 Al formed by the ARB process was thermally stable up to 200°C [14].

AA3003 alloy has been widely used for moderate strength application requiring good workability [16]. Our previous study has shown that even 250°C/5 min annealing during the ARB process decreased the microhardness, and increased the grain sizes to some extent [11]. This study will examine the nature of microstructural stability in the ARBed 3003 alloy at different annealing condition, for the practical application of this material in the future.

2. Experimental procedures

The experiments were conducted on an Al-Mn 3003 alloy whose chemical composition was shown in Table I. Fully annealed 3003 sheets with the initial grain size of 10.2 μm were prepared. Pieces were cut from the initial plate to dimensions of $1 \times 30 \times 300\ \text{mm}^3$, and they were deformed by the ARB process at 250°C [11]. After the ARB process was repeated up to 8 cycles with an equivalent true plastic strain of 6.4 [13], the deformed sheets were annealed in oil bath or salt bath at temperature of 250–400°C for 1 h, or at 250°C for various times.

The values of Hv represent the average of seven separate measurements taken at randomly selected points using a load of 200 g for 15 s. The tensile specimens were machined from the rolled sheets according to the ASTM E8M standard, oriented along the rolling direction. The gauge length was 25 mm. Tensile tests were

*Author to whom all correspondence should be addressed.

TABLE I Chemical composition of AA3003 alloy (mass%)

Elements	Si	Fe	Cu	Mn	Mg	Cr	Zn	Ti	Al
Content	0.286	0.560	0.118	1.039	0.046	0.006	0.000	0.031	bal.

conducted at room temperature on a standard universal testing machine at the strain rate of 8.3×10^{-4} s^{-1}.

The optical examination of the samples was conducted under conditions of polarized light. Etching was carried out electrolytically using Baker's solution of 5 ml HBF_4 and 200 ml distilled water and a stainless steel cathode. All optical microstructures were observed along the transverse direction of the rolling samples.

Specimens were also examined using a JEM-2000 FX II transmission electron microscope (TEM) operating at 200 kV. Thin foils parallel to the rolling plane were prepared by a twin jet electro-polisher using a solution of 140 ml HNO_3 and 280 ml CH_3OH. Selected area electron diffraction (SAD) patterns were taken from regions having diameters of 3 μm. Measurements of the grain size were made directly from the TEM photomicrographs or optical micrographs using an Image & Microscopy Program. At least 100 different grains in every condition were chosen.

3. Results

3.1. Microstructure

Other researchers [9, 10] showed that most of subgrain boundries are transformed to high angle boundaries in several ARB cycled commercial purity aluminum alloy sheets, which had to be measured the local boundary orientations by Kikuchi analysis. But the spot pattern analysis is another simple method to evaluate those trends. According to our previous paper on the several cycle ARB processed 3003 alloy sheets [11], most of the SAD patterns showed single net patterns after 3 cycles. This means most of the specimen still had subgrain structure at this stage. But some regions showed scattered diffraction patterns that show the existence of ultra-fine grain with high angle boundaries. The fraction of the ultra-fine grains increased with the cycles. After 8 cycles, all the SAD patterns showed the presence of high angle grain boundaries due to the distribution of diffraction spots around circles. This means that most of grain boundaries in the 8-cycle ARB processed 3003 alloy sheets consisted of high angle grain boundaries along the normal direction to rolling plane. Therefore, the microstructure having ultra fine grain size about 0.65 μm was formed in this condition.

Similar with that of as-fabricated material, the grain sizes of the ARBed specimens after annealing at 250°C

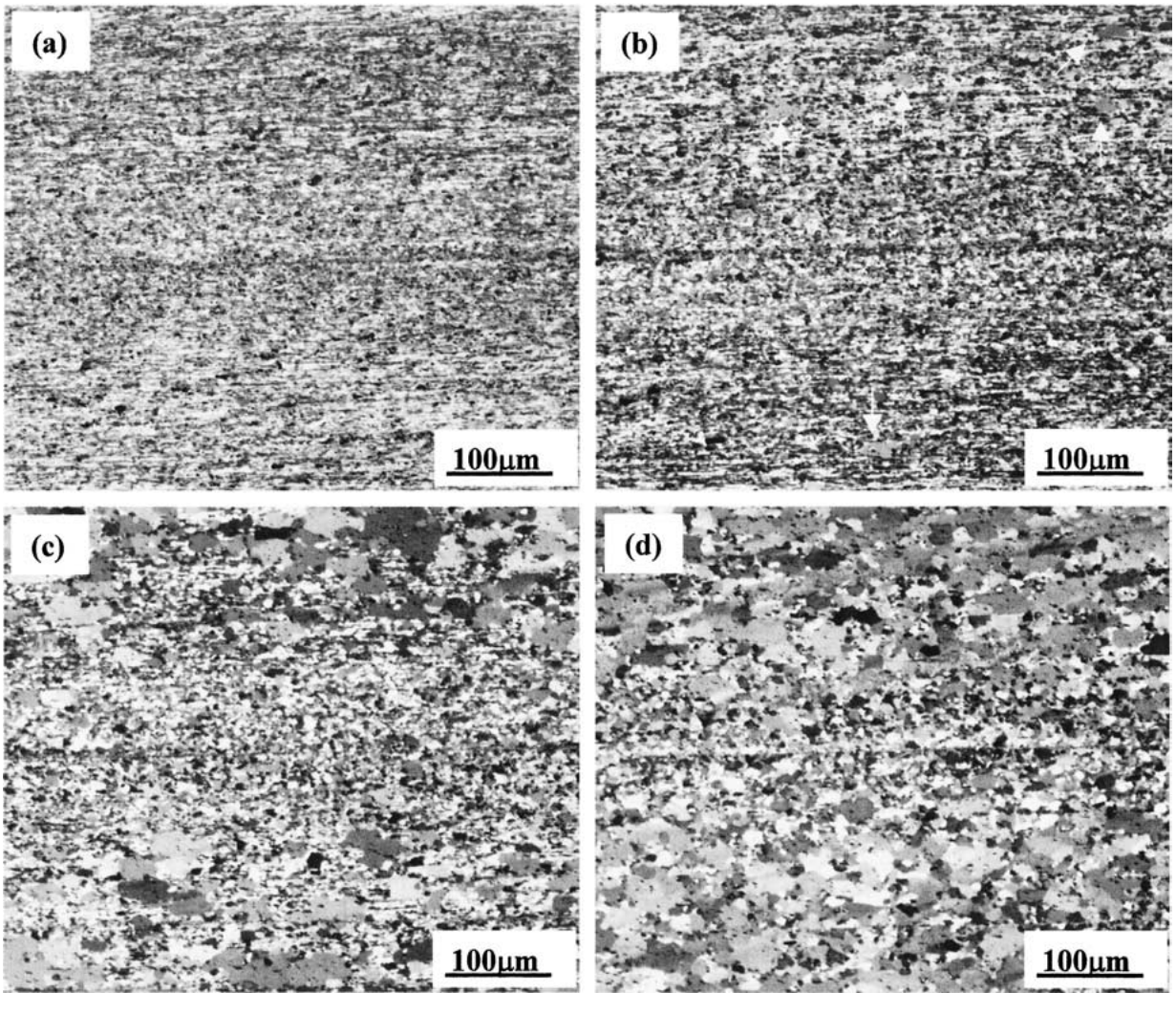

Figure 1 Optical microstructure of the ARBed 3003 alloy after annealing at different temperature for 1 h: (a) 275°C/1 h, (b) 300°C/1 h, (c) 350°C/1 h, and (d) 400°C/1 h.

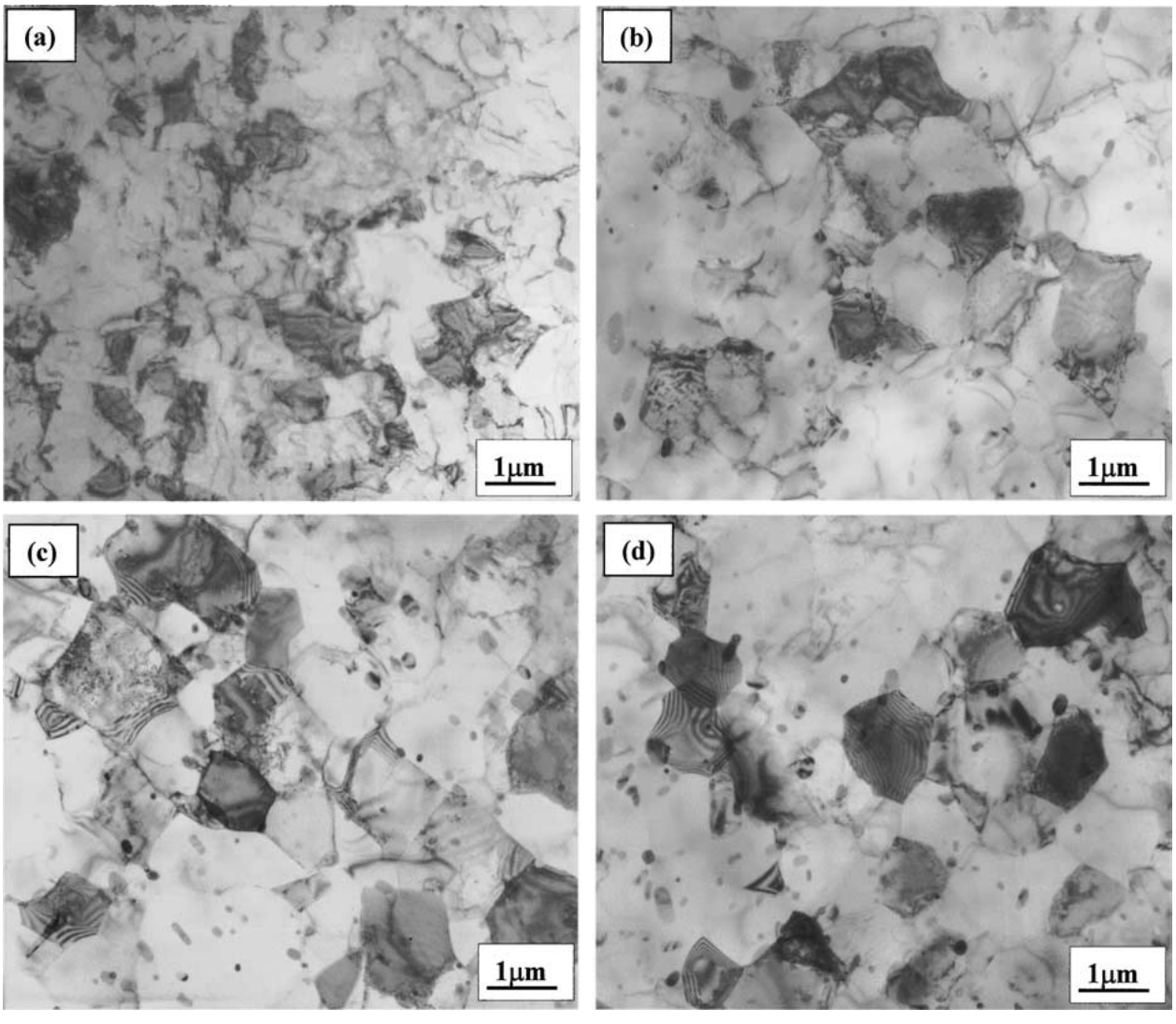

Figure 2 TEM micrographs of the ARBed 3003 alloy after annealing at 250°C for various times: (a) as-ARB, (b) 250°C/1 h, (c) 250°C/5 h, and (d) 250°C/10 h.

for 5 min to 10 h cannot distinguish by optical micrographs. However, with increasing the annealing temperature above 300°C, they can be seen gradually by optical micrographs. Fig. 1 shows the optical micrographs of the ARBed specimens after annealing at different temperature for 1 h. Only a few coarse grains (See arrows in Fig. 1b) appeared in some regions of the 300°C annealing samples. After 350°C annealing (Fig. 1c), most fine grains formed in the ARB process were transformed to coarse grains (average size ∼20 μm). This process was finished after 400°C (Fig. 1d).

Fig. 2 demonstrates the TEM microstructure of the ARBed samples after annealing at 250°C for various times, and Fig. 3 gives the correspondent changing tendency of the grain size measured in the TEM micrographs. It shows that the average grain size of the ARBed 3003 alloy increased homogeneously and gradually with increasing the annealing times. For example, the average grain size in the as-ARBed specimens was about 0.65 μm, while that of the 1 h-annealing specimens was about 1 μm, and that of the 10 h-annealing specimens was about 1.5 μm.

The variation of the grain sizes of the ARBed samples after annealing at different temperature for 1 h is given in Fig. 4. The fine grains grew gradually from as-

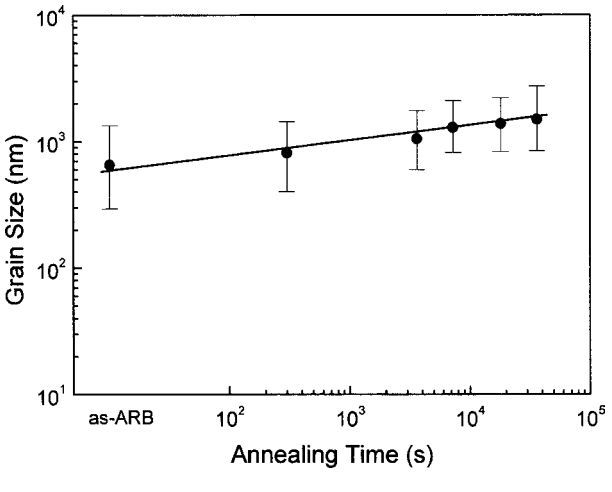

Figure 3 Variation of grain sizes of the ARBed 3003 alloy with increasing the annealing time at 250°C.

fabricated state (∼0.65 μm) to 275°C-annealing state (1.69 μm). After that, bimodal distribution of the grain size appeared due to the coexistence of fine grains and coarse grains. But in the 300 and 325°C samples, the most areas were still filled with ultra fine grains. Some fine grains grew gradually with further increasing the

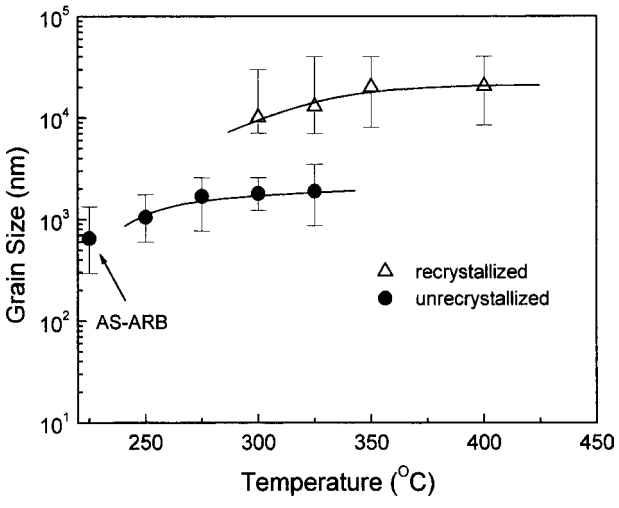

Figure 4 Variation of grain sizes of the ARBed 3003 alloy with increasing the annealing temperature for 1 h.

annealing temperature, and the area fraction of the coarse grains increased with the annealing temperature. After 400°C annealing, all the fine grains were transferred to coarse grains with the average grain size of 20.5 μm. The change of the grain sizes can also be seen in the TEM micrograph of Fig. 5 and optical micrograph of Fig. 1.

3.2. Mechanical properties

Fig. 6 presents the variation of the Vickers microhardness of the ARBed 3003 alloy after annealing with increasing annealing times at a constant temperature (Fig. 6a) and as a function of temperature for one hour (Fig. 6b). In the as-ARBed state, the Vickers microhardness value was ~77.7. After annealing at 250°C for only 1 min, the microhardness value decreased by ~20%. Then it decreased slightly with increasing the annealing time at the same temperature (Fig. 6a). After annealing at 250°C for 1 h, the microhardness value decreased greatly, from 77.7 to 54.5 (Fig. 6b). Then the microhardness decreased continually until 400°C except the small sudden drop after 325°C. After annealing at 400°C for 1 h, the microhardness decreased to 38.5, which is the same with the value of initial material before ARB process [11].

The ambient tensile properties of ARBed 3003 alloy after annealing at 250°C for various annealing times are presented in Fig. 7. It can be seen that tensile strength (UTS) and yield strength (YS) decreased significantly after annealing at 250°C for 5 min, and then the strengths remained nearly unchanged until the annealing time of 5 h. After annealing for 10 h, the strengths decreased again. On the other hand, with increasing annealing time, the elongation kept a constant value of about 5% until the annealing time of 5 h. After annealing for 10 h, the elongation increased suddenly to ~20%.

Fig. 8 presents the stress-strain curves of the samples at different conditions. As similar to the tensile behavior of UFG materials reported previously [15, 17], as-ARBed, 250°C and 275°C-annealed samples exhibited a narrow (or no) strain hardening behavior. While, the fully annealed sample at 400°C for 1 h exhibited the typical strain hardening behavior with large elongation.

Fig. 9 presents the microhardness versus $d^{-1/2}$ (grain size) dependence characteristic of the ARBed 3003 alloy. The Hall-Petch dependence was observed after annealing, but the slope of this dependence was changed. The curve has been divided into three parts, marked by A, B, C zone, respectively, as shown in Fig. 9. The microhardness decreased significantly with increasing grain size before annealing for 5 min at 250°C (A zone), and annealing after 275°C for 1 h (C zone). The microhardness also decreased slightly with increasing grain size between A and C zone (B zone).

4. Discussion

4.1. Continuous recrystallization

It is recognized that ultra fine grain structure can evolve homogeneously and gradually during the annealing of severely deformed metals. This phenomenon was referred variously to as "extended recovery," "*in-situ*

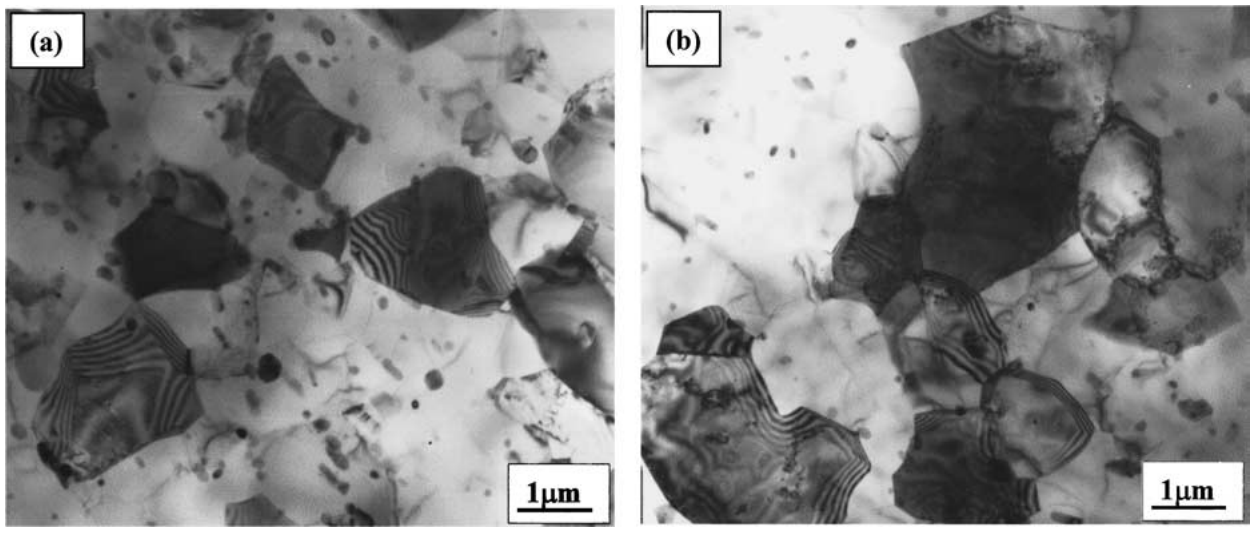

Figure 5 TEM micrographs of the ARBed 3003 alloy after annealing at different temperature for 1 h: (a) 275°C/1 h and (b) 325°C/1 h.

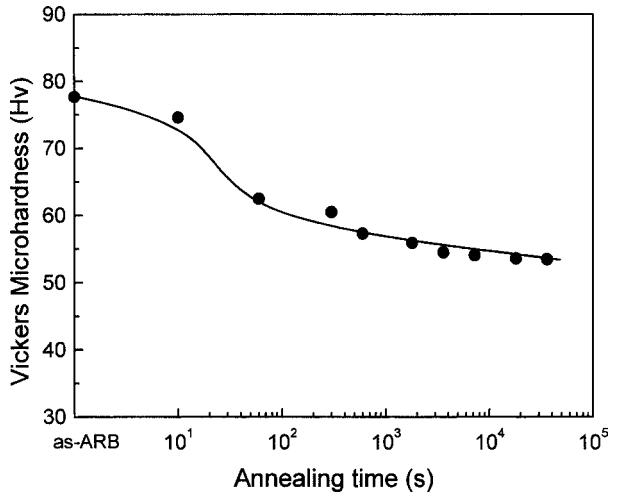

(a)

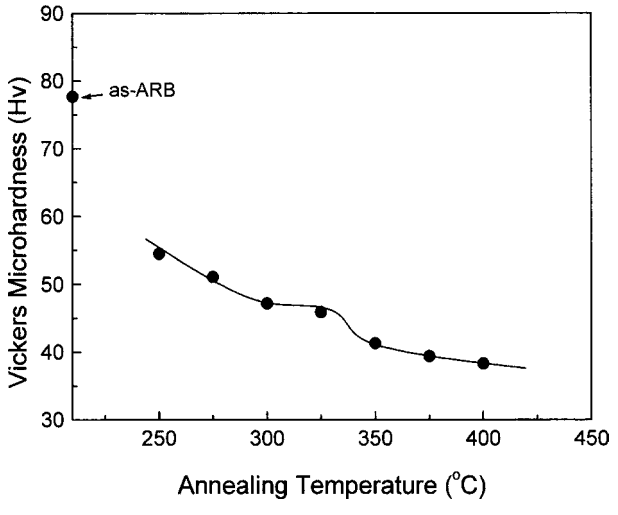

(b)

Figure 6 Variation of Vickers microhardness of the ARBed 3003 alloy with increasing the annealing time at 250°C (a), and with increasing the annealing temperature for 1 h (b).

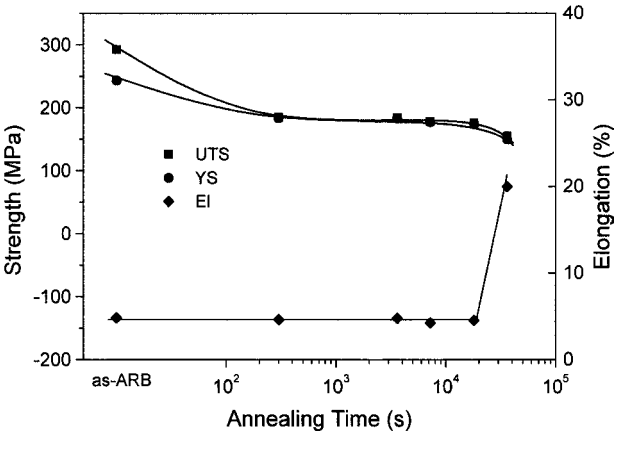

Figure 7 Variation of ambient tensile properties of the ARBed 3003 alloy with increasing the annealing time at 250°C.

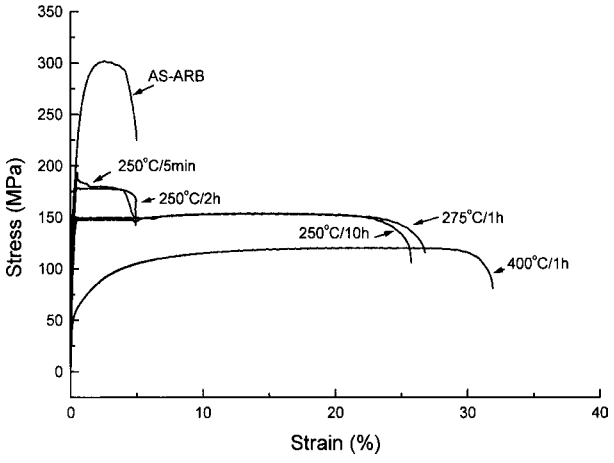

Figure 8 Stress-strain curves of ARBed 3003 alloy at different conditions.

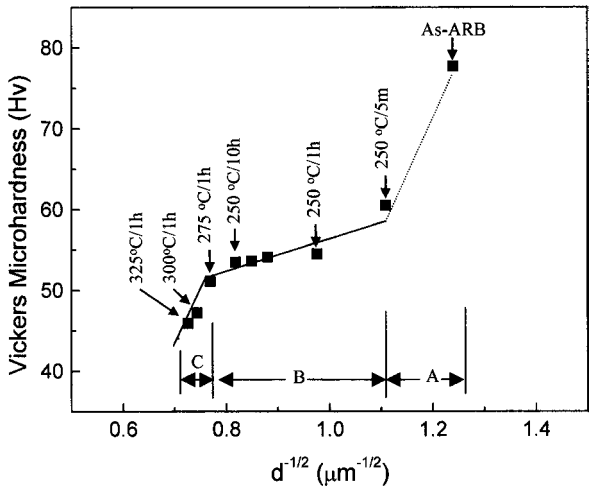

Figure 9 Microhardness versus the mean grain size in the ARBed 3003 alloy.

recrystallization," and "continuous recrystallization" (the most widely used) [18, 19]. As seen in the previous works [11], high angle GBs were formed in all the specimens of 3003 alloy after 6 cycles of ARB. In this study, the grains grew homogeneously and gradually during the annealing process below the annealing temperature of 275°C. This means high angle GBs moved continuously in this process. So this reaction should be referred to as continuous recrystallization. Continuous recrystallization is usually observed frequently in alloys rather than in pure metals [19], often at relatively lower temperature. With increasing the annealing temperature up to 300°C, discontinuous recrystallization took place in some areas of the alloy (Fig. 1b). After annealing at 400°C, discontinuous recrystallization happened in nearly all the areas (Fig. 1d).

From above study, it can be seen that the UFG (≤ 1 μm) formed in the highly deformed 3003 alloy can be stable until annealing at 250°C for 1 h, and the fine grains (<2 μm) can be stable until annealing at 275°C for 1 h by a large number of fine dispersoids such as Al_6Mn. Therefore, grain structure in the ARBed 3003 alloys after intense plastic strain is reasonably stable.

4.2. The change of microhardness versus grain size

To analyze the nature of the observed dependence of the microhardness on $d^{-1/2}$ (Fig. 9), it would be interesting to study the microstructure of the alloy at

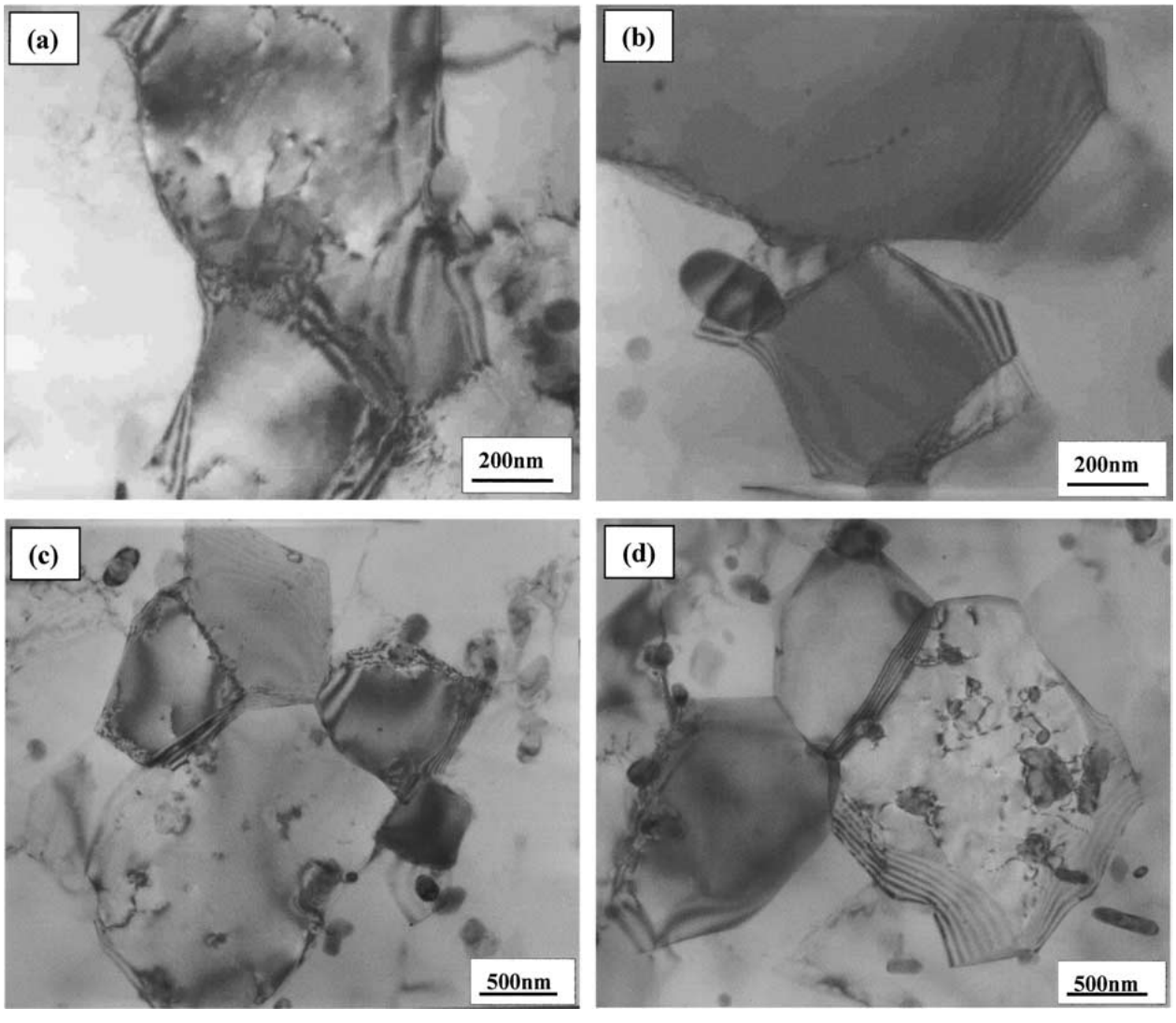

Figure 10 Higher magnification of TEM micrographs of the ARBed 3003 alloy after annealing at different conditions: (a) as-ARB, (b) 250°C/5 m, (c) 250°C/10 h, and (d) 325°C/1 h.

different conditions. As in the previous works [11], it has been observed that UFG microstructure with high angle boundaries was formed after 6 cycles of ARB process. From Fig. 10a, it can be seen the higher magnification TEM micrographs of the as-ARBed specimen. It shows a typical feature of deformed GBs with the occurrence of extinction contours inside grains, which are linked with elastic stresses originated from GBs. These deformed GBs possess a higher energy and long-range stresses, and has been observed in different UFG materials [3, 20–22]. In this state, the hardness is very high because of high dislocation density and large strain field.

After annealing at 250°C for 5 min, the usual equilibrium GBs with a typical banded contrast and relatively few dislocations in the grains formed in most grains of the materials, as shown in Fig. 10b. After annealing at 250°C for 1 h, the whole volume of the material was filled with stable straightened GBs and low dislocation density in grain (Fig. 10c). Therefore, the significant decrease of the microhardness during the A zone in Fig. 9, is mainly attributed to the transformation from deformed GBs to the stable straightened GBs by annihilation of stress field, and the grain growth has only a little effect on it. Other works about the UFG materials [3, 20, 21] also confirmed this phenomenon.

With further increasing the annealing time up to 10 h at 250°C, and increasing annealing temperature to 275°C (B zone), the grains grew continuously in this zone (continuous recrystallization process). So the Hall-Petch dependence kept a constant value during this period. But the decrease of the microhardness versus grain size during this zone is very slow. The Hall-Petch relation slope change after annealing is also observed in other UFG materials due to the reduction of dislocation density and stress field [17, 23, 24].

With further increasing the annealing temperature up to 325°C, the Hall-Petch relation slope changed greatly, and the hardness decreased significantly with the grain size. In this period, bimodal grain sizes began to appear. The real average grain size was difficult to provide in this state, and only the continuous recrystallized grain size was given in Fig. 9. Though in this period, the most areas of the materials were filled with the continuous recrystallized grains, but the effect of discontinuous recrystallized grains on the hardness should not ignore fully. This may be ascribed to the much decrease of hardness of these samples.

4.3. Tensile deformation behavior

The fully recrystallized material (400°C/1 h annealing) exhibited the typical strain hardening behavior (Fig. 8), and its deformation behavior was the same with other conventional materials. For the as-ARBed material, strain hardening behavior also happened, but it was in a narrow strain range (~2%), then the material tended to break. So it possessed a high strength and low ductility. As discussed in last section, high dislocation density and small grain size may play a main role in this deformation behavior. An additional annealing (250–275°C) changed the GB condition of this material from deformed state to a stable state, and grains grew gradually and continuously. Therefore, the mechanical behaviors of 250–275°C annealing samples were very different with those of conventional materials. They exhibited a narrow (or no) strain-hardening region followed by stable flow at a very low strain hardening rate. Especially for the 250°C/10 h and 275°C/1 h sample, this stable process is very long, and led to a high ductility (>20%). But their yield strength were about three times of fully recrystallized material (400°C/1 h). These characteristics are very similar to those UFG materials fabricated by ECA pressed copper and low carbon steel alloys [15, 17]. Since 250–275°C annealed materials exhibited little (or no) strain-hardening behavior, the dislocation pile up mechanism could not explain its high strength. A dislocation bow-out model, which usually explains the mechanical behavior of nanocrystalline materials, would applicable to the present experimental results [15, 17]. However, a quantitative measurement of the dislocation density need perform. These works need further study.

5. Conclusions

1. The grain size of the ARBed 3003 alloy increased homogeneously and gradually with increasing the annealing time at 250°C and increasing the annealing temperature up to 275°C for 1 h. These reactions were referred to as continuous recrystallization reactions. The process that coarse grains grew suddenly in some regions after 300°C annealing for 1 h, was referred as discontinuous recrystallization reactions.

2. The Hall-Petch dependence was observed in the plot of microhardness versus $d^{-1/2}$ of the ARBed 3003 alloy, but its dependence slope of this alloy was changed due to the internal stress field and grain size.

3. The materials annealed at 250–275°C exhibited an unusual tensile behavior, with a narrow (or no) strain hardening regions followed by a long stage stable flow, similar to other UFG materials.

4. The UFG ($\leq$1 μm) formed in the ARBed 3003 alloy can be stable until annealing at 250°C for 1 h, and the fine grains (<2 μm) can be stable until annealing at 275°C for 1 h. Therefore, grain structure formed in the ARBed 3003 alloys after intense plastic strain is reasonably stable.

References

1. J. RICHERT and M. RICHERT, *Aluminium* **62** (1986) 604.
2. R. Z. VALIEV, R. R. MULYUKOV, V. V. OVCHINNIKOV and V. A. SHABASHOV, *Scr. Mater.* **25** (1991) 2717.
3. R. Z. VALIEV, N. A. KRASILNIKOV and N. K. TSENEV, *Mater. Sci. Eng.* A **137** (1991) 35.
4. Y. IWAHASHI, Z. HORITA, M. NEMOTO and T. G. LANGDON, *Acta Mater.* **45** (1997) 4733.
5. Y. SAITO, N. TSUJI, H. UTSUNOMIYA, T. SAKAI and R. G. HONG, *Scr. Mater.* **39** (1998) 1221.
6. Y. SAITO, H. UTSUNOMIYA, N. TSUJI, T. SAKAI and R. G. HONG, *J. Japan Inst. Metals* **63** (1999) 790.
7. Y. SAITO, H. UTSUNOMIYA, N. TSUJI and T. SAKAI, *Acta Mater.* **47** (1999) 579.
8. N. TSUJI, Y. SAITO, H. UTSUNOMIYA and S. TANIGAWA, *Scr. Mater.* **40** (1999) 795.
9. X. HUANG, N. TSUJI, N. HANSEN and Y. MINAMINO, *Mater. Sci. Eng.* A **340** (2003) 265.
10. *Idem.*, *Mater. Sci. Forum* **408–412** (2002) 715.
11. Z. P. XING, S. B. KANG and H. W. KIM, *J. Mater. Sci.* **37** (2002) 717.
12. *Idem.*, *Scr. Mater.* **45** (2001) 597.
13. *Idem.*, *Metall. Mater. Trans.* A **33A** (2002) 1521.
14. K. T. PARK, H. J. KWON, W. J. KIM and Y. S. KIM, *Mater. Sci. Eng.* A **316** (2001) 145.
15. K. T. PARK, Y. S. KIM, J. G. LEE and D. H. SHIN, *ibid.* **293** (2000) 165.
16. J. R. DAVIS, "ASM Specialty Handbook: Aluminium and Aluminium Alloys" (ASM International, Materials Park, Ohio, 1993) p. 33.
17. R. Z. VALIEV, E. V. KOZLOV, Y. F. IVANOV, J. LIAN, A. A. NAZAROV and B. BAUDELET, *Acta Mater.* **42** (1994) 2467.
18. R. D. DOHERTY, D. A. HUGHES, F. J. HUMPHREYS, J. J. JONAS, D. J. JENSEN, M. E. KASSNER, W. E. KING, T. R. McNELLEY, H. J. McQUEEN and A. D. ROLLETT, *Mater. Sci. Eng.* A **238** (1997) 219.
19. F. J. HUMPHREYS, *Acta Mater.* **45** (1997) 5031.
20. R. Z. VALIEV, A. V. KORZNIKOV and R. R. MULYUKOV, *Mater. Sci. Eng.* A **168** (1993) 141.
21. R. SH. MUSALIMOV and R. Z. VALIEV, *Scr. Metall. Mater.* **12** (1992) 1685.
22. J. T. WANG, M. FURUKAWA, Z. HORITA, M. NEMOTO, R. Z. VALIEV and T. G. LANGDON, *Mater. Sci. Eng.* A **216** (1996) 41.
23. G. E. FOUGERE, J. R. WEERTMAN, R. W. SIEGEL and S. KIM, *Scr. Metall. Mater.* **26** (1992) 1879.
24. J. LANGUILLAUME, F. CHMELIK, G. KAPELSKI, F. BORDEAUX, A. A. NAZAROV, G. CANOVA, C. ESLING, R. Z. VALIEV and B. BAUDELET, *Acta Mater.* **41** (1993) 2953.

Received 30 March
and accepted 10 October 2003